

# I. HEAVY-ION NUCLEAR PHYSICS RESEARCH

## OVERVIEW

This research involves investigating the structure, stability, reactions and decays of nuclei. This information is crucial for understanding the evolution of the universe, the workings of stars and the abundances of the elements that form the world around us. The forefront area of research is investigating the properties of nuclei which lie very far from stability, and which are critical in understanding nucleosynthesis. Most of our research is based at the Argonne Tandem-Linac Accelerator (ATLAS), a national heavy-ion user facility. Programs are also mounted at the Relativistic Heavy Ion Collider (RHIC), at the 88" cyclotron at Berkeley and at other forefront facilities. The major thrusts of the program are: a) deepening and generalizing our understanding of nuclear structure to allow a reliable description of all bound nuclear systems, b) studying the reactions which are important in the cataclysmic events in the cosmos which lead to the synthesis of the chemical elements, c) testing the limits of the Standard Model, the fundamental theory that currently best represents our understanding of the laws and fundamental symmetries of nature.

The specific research topics we are pursuing include the studies of transfermium nuclei ( $Z > 100$ ) with a goal of studying the very heaviest nuclei, the study of the shapes and stability of nuclei along the proton dripline, the effects of deformation on proton radioactivity, the production and acceleration of short-lived nuclei and their use in measurements of reactions which are important in astrophysics, and the high-precision measurement of nuclear masses. In addition, there are complimentary efforts in the use of Accelerator Mass Spectrometry (AMS) for environmental research; in the investigation of nuclear matter at relativistic energies; and in the dynamics of cooled ions confined in storage rings or traps. The ATLAS-based research exploits the unique capabilities of the accelerator, both in the stable beam program, and in production of accelerated beams of short-lived isotopes. The experiments employ state-of-the-art research equipment, including the Fragment Mass Analyzer (FMA), a large solid angle silicon array, "Ludwig", and the Canadian Penning Trap, (CPT) which is operating at ATLAS. Several new detector initiatives are being pursued including the return of Gammasphere to ATLAS, upgrading the FMA and its focal plane counters, refining the "In-Flight" radioactive beam facility and its detector systems, and constructing the Advanced Penning Trap (APT). Considerable effort continues in developing the next generation gamma ray detectors with "tracking" capability. Intensive participation in the PHOBOS experiment at Brookhaven has continued.

Some of the specific goals of the program can be summarized as follows:

- Develop and utilize beams of short-lived nuclei,  ${}^8\text{Li}$ ,  ${}^8\text{B}$ ,  ${}^{14}\text{O}$ ,  ${}^{17,18}\text{F}$ ,  ${}^{20,21}\text{Na}$ ,  ${}^{25}\text{Al}$ ,  ${}^{37}\text{K}$ ,  ${}^{44}\text{Ti}$ ,  ${}^{56}\text{Ni}$ , and others, to improve the understanding of reactions of astrophysical importance. Emphasis has focused on “in-flight” production of short-lived ion-species using kinematically inverse reactions on light gaseous targets. Considerable scope still remains for further improving the intensity and quality of these beams in the future.
- Study the structure, stability, and modes of excitation and decay of the heaviest elements and study of the reaction mechanisms through which they can be synthesized. This research has many facets, including exploring the opportunities for producing the very heaviest nuclei ( $Z > 106$ ), studies of isomeric decays, studies of “fine-structure” in the alpha decay of heavy elements, and “inbeam” spectroscopy and calorimetry.
- Study the shapes, stability and decay modes of nuclei along the proton dripline in order to improve understanding of partially bound nuclei. Study proton tunneling through deformed barriers, in order to increase the spectroscopic information obtained through proton radioactive decay rates. Study the influence of vibrations and coupling to other nucleons in odd-odd systems to generalize the understanding of proton radioactivity.
- Make high-precision measurements of nuclear masses with the CPT, particularly the masses of  $N = Z$  nuclei which are of astrophysical interest and are important for testing CVC theory, and measuring the masses of neutron fission fragments which lie close to the anticipated r-process path. Improve the efficiency for production, separation, cooling, transportation, and trap loading of ions to increase sensitivity.
- Develop position sensitive germanium detectors, for “tracking” gamma rays in order to allow the imaging of the source of radiation. The ANL focus is on developing planar germanium wafer technologies, in parallel with involvement in national plans to construct a  $4\text{-}\pi$  germanium shell, following the GRETA concept.
- Investigate the collisions and deconfinement of nucleons in nuclear matter at very high temperatures and densities that are achieved in relativistic heavy-ion collisions of gold nuclei at 200 GeV/u. Our participation is using the PHOBOS detector at the RHIC accelerator at Brookhaven National Laboratory.
- Perform detailed R&D studies for the Rare Isotope Accelerator (RIA) and participate in all efforts to refine the designs for the accelerators, target stations, post accelerator, and experimental equipment. Intense effort is being directed to development of the “gas catcher” technology for cooling primary beams.

## A. REACTIONS OF ASTROPHYSICAL IMPORTANCE USING STABLE AND RADIOACTIVE BEAMS

The “in-flight” technique for producing radioactive beams using reactions in inverse kinematics continues to evolve and be refined. Studying reactions involving these exotic beams helped clarify and quantify some reaction processes like the “breakout” from the hot CNO cycle and the beginning of the more explosive rp-process. Recent beams that were developed and used for physics projects now include:  ${}^8\text{Li}$  ( $t_{1/2} = 842$  ms),  ${}^8\text{B}$  ( $t_{1/2} = 770$  ms),  ${}^{14}\text{O}$  ( $t_{1/2} = 70.6$  s),  ${}^{17}\text{F}$  ( $t_{1/2} = 65$  s),  ${}^{20}\text{Ne}$  ( $t_{1/2} = 446$  ms),  ${}^{21}\text{Ne}$  ( $t_{1/2} = 22.5$  s),  ${}^{25}\text{Al}$  ( $t_{1/2} = 7.2$  s), and  ${}^{37}\text{K}$  ( $t_{1/2} = 1.22$  s). The reconfigured radioactive ion production beam line, which now includes a large-bore solenoid, was tested and successfully used in experiments. In addition to the ATLAS projects with accelerated radioactive beams, several more conventional heavy-ion reaction studies produced data on nuclei critical to the rp-nucleosynthesis path. A significant opportunity lies in studying compound nuclear states near the  $(p,\gamma)$  reaction threshold, populated with near-barrier fusion of heavy ions, and spectroscopically investigated using Gammasphere. This technique seems to have many possibilities, as it is excellent for precisely determining the excitation energy of levels and their angular momentum properties.

### a.1. Determination of the ${}^8\text{B}$ Neutrino Spectrum (J. P. Schiffer, K. E. Rehm, I. Ahmad, J. Greene, A. Heinz, D. Henderson, R. V. F. Janssens, C. L. Jiang, E. F. Moore, G. Mukherjee, R. C. Pardo, T. Pennington, G. Savard, D. Seweryniak, G. Zinkann, W. T. Winter,\* S. J. Freedman,\* and M. Paul†)

The solar neutrino “problem” originated in 1968 when the Homestake  ${}^{37}\text{Cl}$  capture experiment placed a limit on the solar neutrino flux that was less than half of solar model predictions. Additional solar neutrino data have since been collected by the Gallex, SAGE, and GNO  ${}^{71}\text{Ga}$  capture experiments and the Kamiokande, Super-Kamiokande, and Sudbury Neutrino Observatory (SNO) water Cherenkov experiments.

Neutrinos from the  $\beta$ -decay of  ${}^8\text{B}$ , produced in the solar core, account for 80% of the  ${}^{37}\text{Cl}$  capture events, and Super-Kamiokande and SNO are sensitive to the differential  ${}^8\text{B}$  neutrino spectrum. A determination of the physics of leptonic flavor mixing from the solar neutrino data requires an understanding of the  $\alpha$ -decay of  ${}^8\text{B}$  into  ${}^8\text{Be}$ , which depends strongly on the energy profile of the unstable  ${}^8\text{Be}$ , which must be determined experimentally.

Previous measurements of the  $\alpha$ -spectrum involved the production of  ${}^8\text{B}$  ( $t_{1/2} = 778$  ms) which was stopped in a catcher foil and positioned adjacent to a Si detector. Energy deposition in the detector was measured and corrections were made for energy

losses in the catcher foil and detector dead layer. The first experiments, by Farmer and Class,<sup>1</sup> De Braekeleer and Wright,<sup>2</sup> and Wilkinson and Alburger,<sup>3</sup> observed the singles  $\alpha$ -spectrum. Data from these measurements differ from each other by energy offsets of order 100 keV, an effect attributed to systematic problems with detector calibration and energy loss in the dead layer.

Additional information on the  ${}^8\text{B}$   $\beta$ -decay is provided by the  $\beta$ -spectrum which, like the neutrino spectrum, is altered by the broad  ${}^8\text{Be}$  resonance. A precise measurement of the  $\beta$ -spectrum above 9 MeV was performed using a  $180^\circ$  magnetic spectrograph.<sup>4</sup> The singles  $\alpha$ -spectrum data and  $\beta$ -spectrum data were used to predict a neutrino spectrum, based on varying assumptions with the most comprehensive analysis performed by Bahcall *et al.*<sup>5</sup>

Recently, the coincidence  $\alpha$ -spectrum was measured using two detectors resulting in a spectrum quite different from the earlier measurements.<sup>6</sup> Both the Super-Kamiokande and SNO collaborations interpreted their data using the  ${}^8\text{B}$  neutrino spectrum from the most recent coincidence measurement.

We developed an experiment that was designed to minimize systematic effects which may have affected the previous  $\alpha$  measurements. A beam of  $^8\text{B}$  ions was implanted into the center of a planar Si detector, which eliminated energy loss corrections due to catcher foils and detector dead layers and allowed the energy deposited by both  $\alpha$ -particles to be observed with a single detector. Beta-particle energy deposition is unavoidable with this technique, but was minimized by the use of a thin ( $91\ \mu\text{m}$ ) Si detector, sufficient to stop the most energetic  $\alpha$ -particles, and by the requirement of a  $\beta$  coincidence. For calibration  $^{20}\text{Na}$  ions were implanted into the same detector immediately before the  $^8\text{B}$  measurement. The  $\beta$ -decay of  $^{20}\text{Na}$  proceeds 20% of the time to  $\alpha$ -unstable levels in  $^{20}\text{Ne}$  and provides calibration lines in the region of the  $^8\text{B}$   $\alpha$ -spectrum peak.

The experiment was performed using the ATLAS superconducting linear accelerator at the Argonne National Laboratory. A  $^8\text{B}$  beam was produced with the "In-Flight Technique" using the  $^3\text{He}(^6\text{Li}, ^8\text{B})\text{n}$  reaction. A 36.4 MeV  $^6\text{Li}$  beam was incident on a 3.5 cm long gas cell filled with 700 mbar of  $^3\text{He}$  and cooled to 82 K. The pressure and temperature in the cell were held constant to  $\pm 1\%$ . The  $^8\text{B}$  reaction products were separated from the primary  $^6\text{Li}$  beam with a  $22^\circ$  bending magnet and transported into the focal plane of the Enge Split Pole spectrograph where they were identified with respect to mass, charge, and energy in the gas-filled focal plane detector. The magnetic field in the spectrograph was then adjusted to implant 27.3 MeV  $^8\text{B}$  ions (range  $\approx 45\ \mu\text{m}$ ) into a  $91\ \mu\text{m}$  thick Si detector located adjacent to the gas-filled detector in the focal plane. An 11-mm diameter Ta collimator in front of the Si detector ensured that the  $^8\text{B}$  ions were implanted only into the central region of the detector.

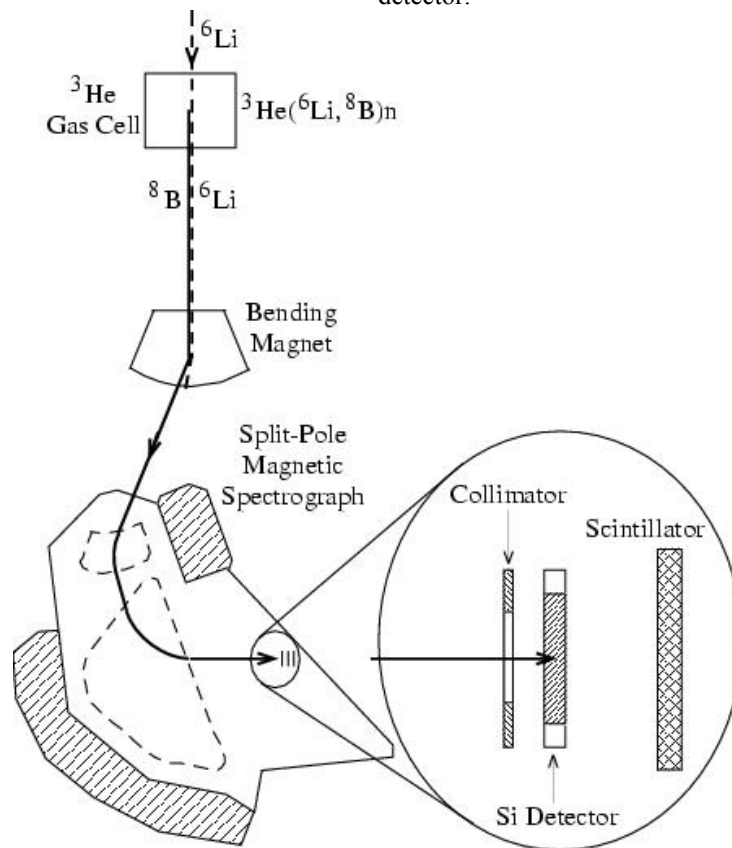


Fig. I-1. Schematic sketch of the experimental apparatus used in the measurement

A 25-mm diameter  $\times$  2-mm thick plastic scintillator coupled by a light guide to a Hamamatsu R647 photo-multiplier tube was positioned 12 mm behind the Si detector. The plastic scintillator, operated in coincidence, selected events where the  $\beta$  trajectory was within  $\approx 40^\circ$  to normal. This provided a sample of events with minimum  $\beta$  energy deposition. The Si/scintillator detector system was cooled to  $-5^\circ\text{C}$ . A schematic representation of the apparatus is shown in Fig. I-1.

The  $^6\text{Li}$  beam was cycled (1.5 sec on/1.5 sec off) and data taken only during the beam-off cycle. With an average  $^6\text{Li}$  current of 60 pA about 3  $^8\text{B}$  ions/sec were implanted. Energy signals and the relative timing between the Si and  $\beta$  detectors were recorded, as well as the timing of the Si signal with respect to

the beam-off cycle. Over three days,  $4.5 \times 10^5$   $^8\text{B}$  events were observed, 16% of which were in coincidence with a  $\beta$  event in the scintillator.

The system was calibrated using a  $^{20}\text{Na}$  ( $t_{1/2} = 448$  ms) beam immediately before the  $^8\text{B}$  run. The  $^{20}\text{Na}$  beam was produced using the same in-flight technique with a 199-MeV  $^{19}\text{F}$  beam via the  $^3\text{He}(^{19}\text{F}, ^{20}\text{Na})2n$  reaction. The spectrograph selected  $^{20}\text{Na}$  ions of 170 MeV, and a Mylar foil in front of the Si detector slowed the  $^{20}\text{Na}$  ions to 85 MeV (range in the Si detector  $\approx 45$   $\mu\text{m}$ ). Data acquisition was identical to the  $^8\text{B}$  runs, but the on-off cycle time was reduced to 1 sec on/1 sec off. With a 0.5 pA  $^{19}\text{F}$  beam, about 8  $^{20}\text{Na}$  decays/min were detected in the Si detector, resulting in  $1.0 \times 10^4$   $^{20}\text{Na}$  events over a one day run. Spectra from the implanted  $^8\text{B}$  and  $^{20}\text{Na}$  are shown in Fig. I-2.

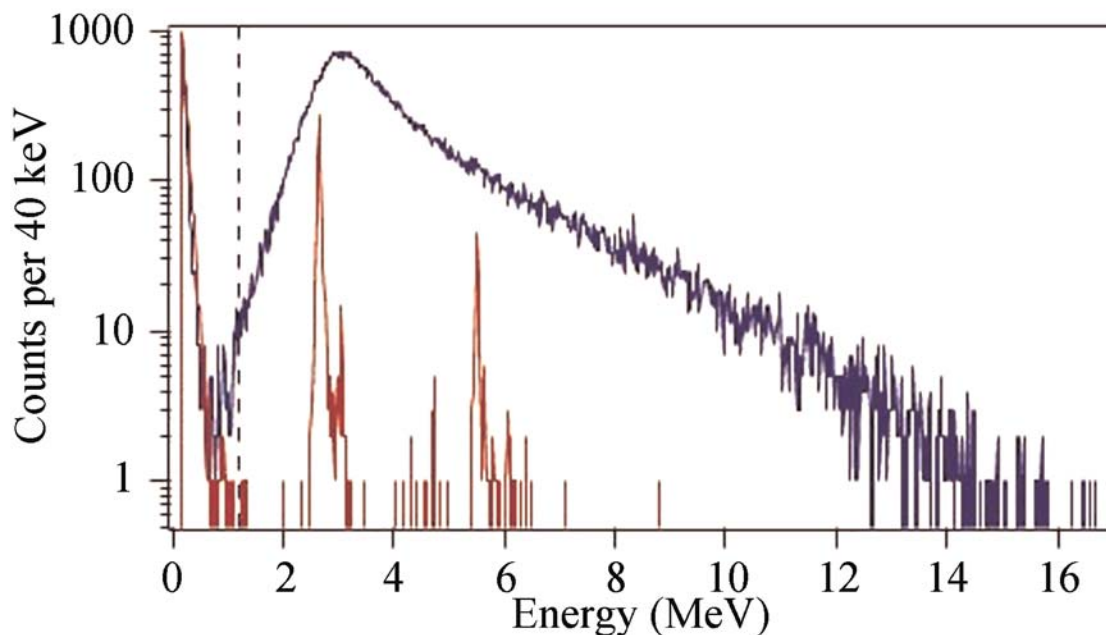


Fig. I-2. The measured alpha-particle spectrum from the decay of  $^8\text{B}$  imbedded in the Si detector is shown in blue, together with the calibration spectrum of alpha particles following the decay of  $^{20}\text{Na}$ , similarly imbedded, in red. The data shown here were in coincidence with the scintillation beta detector to better define the energy deposition from betas in the Si detector

The three largest branches in  $^{20}\text{Na}$  decay provide a good calibration, covering a large fraction of the  $^8\text{B}$  decay spectrum. The pulse-height defect associated with the recoil  $^{16}\text{O}$  nucleus, which carries one fifth of the energy of the alpha disintegration in  $^{20}\text{Na}$  decay,

has been measured for  $^{16}\text{O}$  nuclei in the energy range of interest. The correction is 40-50 keV for the various  $^{20}\text{Na}$  alpha lines.

The detector resolution consists of a noise component and a  $\beta$  energy-loss component. The noise was estimated from the  $^{20}\text{Na}$  peaks and was removed from the  $^8\text{B}$  spectrum. The effect of  $\beta$  energy loss was modeled in a Monte Carlo simulation. The high-energy tail of the  $\beta$  energy deposition spectrum is suppressed by the coincidence requirement. Correction for  $\beta$  energy loss lowered the peak of the coincidence data by 24 keV, as compared to 55 keV for the total data. After the correction, the peaks of the coincidence and total spectra agree within 2 keV.

The recoil energy of the  $^8\text{Be}$  nucleus following the Gamow-Teller  $\beta$ -decay contributes an energy shift of

5 keV at the peak of the alpha spectrum. At the highest alpha energies, contributions from electron capture and a Fermi  $\beta$ -decay branch are significant; however, the recoil effect is  $\leq 0.5$  keV there, which is negligible compared to uncertainties in the energy scale, so these effects can be safely neglected.

The  $\alpha$  spectrum from this measurement is given in Fig. I-3 (blue lines) in comparison with the coincidence measurement from Ref. 6 (red lines). The present result is peaked 53 keV higher in energy than the spectrum by Ortiz *et al.*

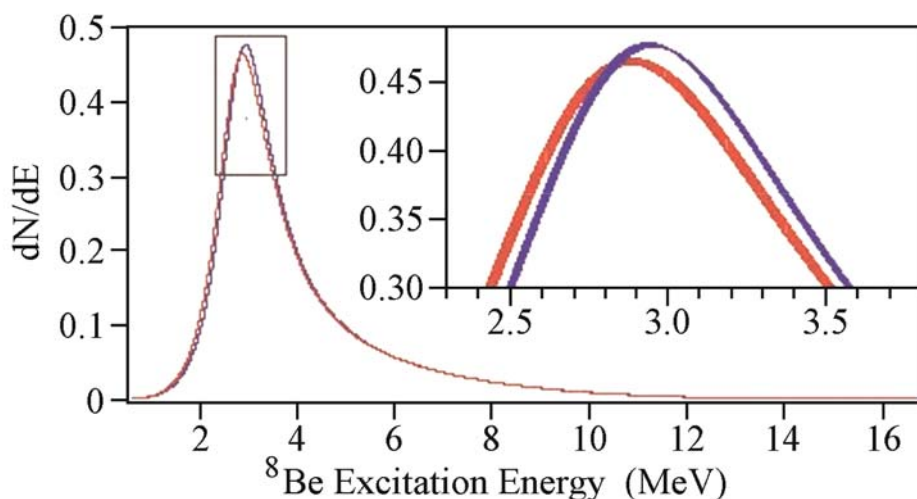


Fig. I-3. Comparison of the measured alpha spectrum from the present measurement, shown in blue, with that of Ortiz *et al.* in Ref. 6 shown in red. The widths of the lines indicate the estimated systematic uncertainties.

The  $^8\text{B}$   $\beta$ -spectrum was deduced from the measured  $\alpha$ -spectrum. Recoil order effects and radiative corrections contribute to the spectrum at the 5% level. The deduced  $\beta$ -spectrum was compared to the experimental spectrum,<sup>4</sup> and gave an agreement of  $\chi^2/\text{dof} = 32.9/31$ , where only statistical uncertainties were included in the minimization function. The calibration uncertainty in the measured  $\beta$ -spectrum is reported in Ref. 5 as 25 keV, and the spectrum deduced here was allowed to float by an energy offset

to mimic the effect of a possible calibration error. Best agreement ( $\chi^2/\text{dof} = 32.5/31$ ) occurs at an offset of  $-13 \pm 20$  keV. The  $\beta$ -spectrum predicted by Ortiz requires a  $-75 \pm 20$  keV offset to produce the best agreement with the data.

A comparison of the  $^8\text{B}$  neutrino spectra recommended by Bahcall *et al.* and Ortiz *et al.* to the spectrum determined here are shown in Fig. I-4.

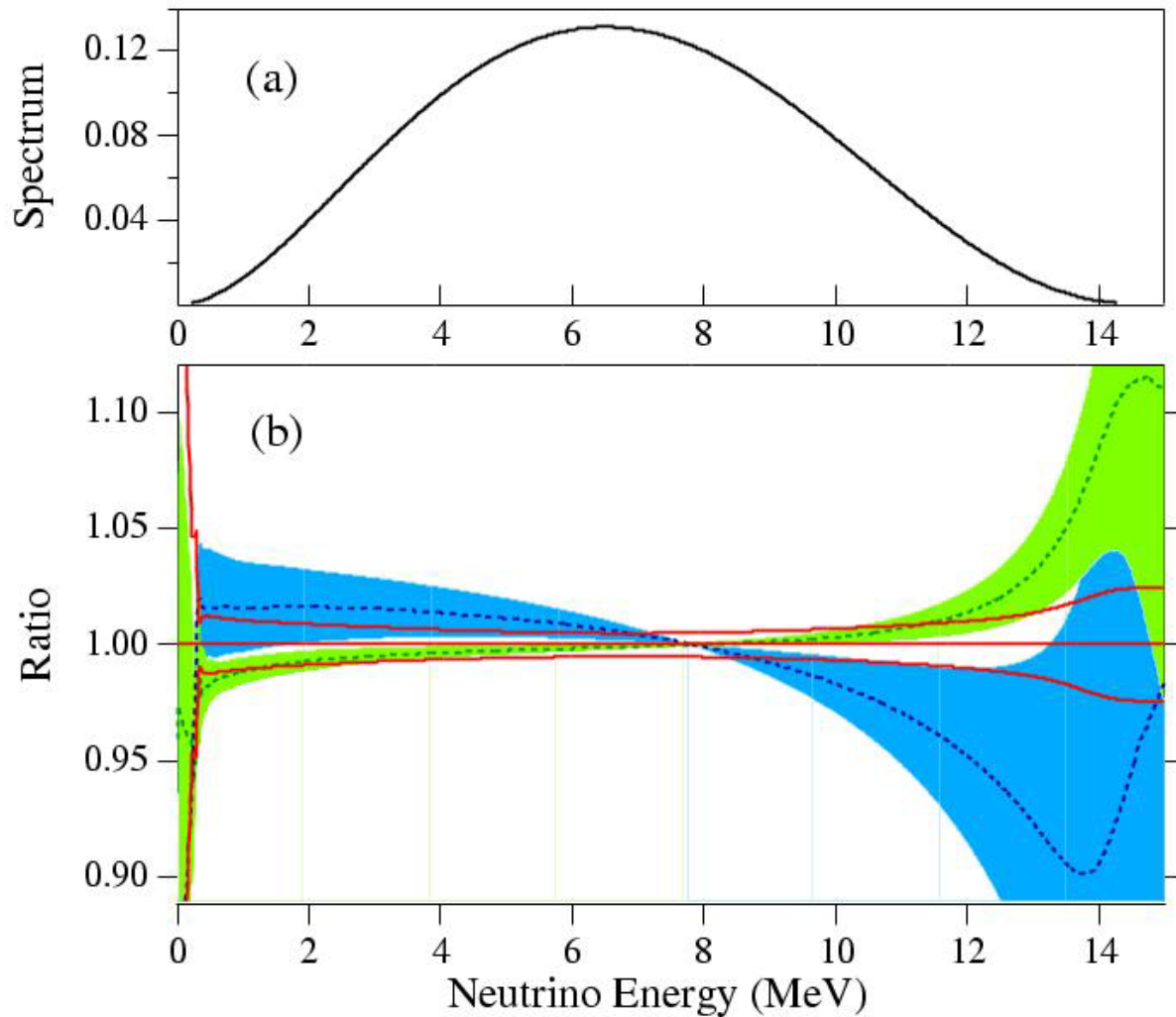


Fig. I-4. The neutrino spectrum deduced from the present measurement is shown in (a). On the bottom the ratio of the neutrino spectrum obtained in Ref. 6 (Ortiz *et al.*) to the present one is shown in green, while that of the spectrum recommended in Ref. 5 from measurements before the work of Ref. 5 (by Bahcall *et al.*) is in blue. The bands indicate 1-sigma errors.

The deviations between the predicted  $^8\text{B}$  neutrino spectra, shown in Fig. I-4, are comparable to the precision with which Super-Kamiokande measured the differential energy spectrum of solar neutrinos.

Interpretation of solar neutrino data will become increasingly dependent on the uncertainties in the neutrino spectrum as the quality of solar neutrino data increases.

\*Lawrence Berkeley National Laboratory and the University of California-Berkeley, †Hebrew University, Jerusalem, Israel.

<sup>1</sup>B. Farmer and C. Class, Nucl. Phys. **15**, 626 (1960).

<sup>2</sup>L. De Braeckeleer *et al.*, Phys. Rev. C **51**, 2778 (1995).

<sup>3</sup>D. Wilkinson and D. Alburger, Phys. Rev. Lett. **16**, 1127 (1971).

<sup>4</sup>J. Napolitano, S. J. Freedman, and J. Camp, Phys. Rev. C **36**, 298 (1987).

<sup>5</sup>J. Bahcall *et al.*, Phys. Rev. C **54**, 411 (1996).

<sup>6</sup>C. Ortiz *et al.* Phys. Rev. Lett. **85**, 2909 (2000).

**a.2. Production of a  $^8\text{Li}$  Beam with the In-Flight Technique** (A. H. Wuosmaa, R. C. Pardo, J. P. Greene, A. Heinz, C. L. Jiang, E. F. Moore, K. E. Rehm, and S. Sinha)

For a planned  $^8\text{Li}(\text{d,p})^9\text{Li}$  experiment we developed  $^8\text{Li}$  ( $T_{1/2} = 0.84$  s) beams with energies between 50 and 75 MeV using the in-flight technique. The  $^8\text{Li}$  beam was produced via the  $\text{d}(^7\text{Li},^8\text{Li})\text{p}$  reaction with a  $^7\text{Li}$  beam from the ATLAS accelerator. The specific rate on target ( $^8\text{Li}$  per sec and per pnA of incident  $^7\text{Li}$  beam) was between 2000 - 2500, independent of the bombarding energy. The contamination from the primary  $^7\text{Li}$  beam was less than 1%. At present the total  $^7\text{Li}$  beam intensity that

can be put on the production target is less than 13 pnA, limited by the radiation monitors of the ATLAS Radiation Interlock System (ARIS). The new Safety Assessment Document which was recently approved, will allow this value to increase by a factor of about 30, which should result in  $^8\text{Li}$  beam intensities of  $\sim 10^6$   $^8\text{Li}/\text{sec}$  on target. With beams of  $\sim 10^6$   $^8\text{Li}/\text{sec}$  the study of the  $^8\text{Li}(\text{d,p})^9\text{Li}$  reaction should be well within the experimental sensitivity.

**a.3. The Branching Ratio  $\Gamma_\alpha/\Gamma_\gamma$  of the 4.033 MeV State in  $^{19}\text{Ne}$**  (K. E. Rehm, A. H. Wuosmaa, C. L. Jiang, J. P. Greene, A. Heinz, D. Henderson, R. V. F. Janssens, E. F. Moore, G. Mukherjee, R. C. Pardo, T. Pennington, J. P. Schiffer, R. H. Siemssen, L. Jisonna,\* M. Paul,† and R. E. Segel\*)

In novae, on accreting neutron stars or in super-massive stars where explosive hydrogen burning occurs, the energy production proceeds via the so-called hot CNO (HCNO) cycle which is a reaction cycle consisting of a sequence of  $(\text{p},\gamma)$ ,  $(\text{p},\alpha)$  reactions and  $\beta^+$  decays:  $^{12}\text{C}(\text{p},\gamma)^{13}\text{N}(\text{p},\gamma)^{14}\text{O}(\text{e}^+\nu_e)^{14}\text{N}(\text{p},\gamma)^{15}\text{O}(\text{e}^+\nu_e)^{15}\text{N}(\text{p},\alpha)^{12}\text{C}$ . In this network, the rate of energy production is limited by the slow  $\beta$  decays of  $^{14,15}\text{O}$  ( $T_{1/2} = 70.6$  s and 123 s, respectively). At higher temperatures ( $T \geq 3.5 \times 10^8$  K), however,  $\alpha$  induced reactions on  $^{14,15}\text{O}$  can bypass these waiting points. This results in a strong increase of the energy production as well as in a breakout from the HCNO into the rapid proton capture (rp) process where, through a sequence of  $(\text{p},\gamma)$  reactions and  $\beta$  decays, nuclei above mass 20 are produced.

There are three pathways for this breakout mechanism:  $^{18}\text{F}(\text{p},\gamma)^{19}\text{Ne}$ ,  $^{15}\text{O}(\alpha,\gamma)^{19}\text{Ne}$  and  $^{18}\text{Ne}(\alpha,\text{p})^{21}\text{Na}$ . The large cross section measured for the  $^{18}\text{F}(\text{p},\alpha)^{15}\text{O}$  reaction leads to a very small branching ratio  $\Gamma_\gamma/\Gamma_\alpha$  and, thus, to a negligible breakout probability through the  $^{18}\text{F}(\text{p},\gamma)$  route. The  $^{18}\text{Ne}(\alpha,\text{p})$  path has the highest Coulomb barrier of the three breakout reactions and it, thus, contributes only at higher temperatures and densities. It is presently assumed that the  $^{15}\text{O}(\alpha,\gamma)$  reaction is the most likely path for a breakout into the rp process.<sup>1</sup>

The astrophysical reaction rate for the  $^{15}\text{O}(\alpha,\gamma)^{19}\text{Ne}$  reaction is dominated by the contribution from the  $3/2^+$  state in  $^{19}\text{Ne}$  at  $E_x = 4.033$  MeV, the first level

above the  $(\alpha,\gamma)$  threshold at 3.529 MeV. We studied the inverse  $^3\text{He}(^{20}\text{Ne},\alpha)^{19}\text{Ne}$  reaction to populate the  $3/2^+$  state in  $^{19}\text{Ne}$  with a 105 MeV  $^{20}\text{Ne}$  beam from the ATLAS accelerator at Argonne National Laboratory. The  $^3\text{He}$  target consisted of a 1.5-mm long gas cell filled with 700 mbar of  $^3\text{He}$  with two 1.5-mg/cm<sup>2</sup> titanium windows. It was cooled to LN<sub>2</sub> temperatures, resulting in an areal density of about 50  $\mu\text{g}/\text{cm}^2$ .

The  $\alpha$  particles from the  $(^3\text{He},\alpha)$  reaction were detected in a Si detector telescope consisting of a 500- $\mu\text{m}$  thick  $32 \times 32\text{-mm}^2$  double-sided silicon-strip  $\Delta E$  detector and a 300- $\mu\text{m}$   $50 \times 50\text{-mm}^2$   $E_{\text{res}}$  detector. The  $\Delta E$  detector was segmented into 32 horizontal and 32 vertical, 1-mm wide, strips.

The coincident  $^{19}\text{Ne}$  particles emitted at an angle  $\theta_{\text{lab}} = 3.7 \pm 1.4^\circ$  were separated from the incident  $^{20}\text{Ne}$  beam with the Enge Split Pole magnetic spectrograph and identified with respect to mass and nuclear charge in the focal plane using a hybrid position-sensitive parallel-plate-avalanche-counter (PPAC) ionization chamber (IC) detector system. Through a measurement of magnetic rigidity, energy, time-of-flight, range and height of the Bragg peak, mass and charge could be determined by two independent methods, resulting in excellent background suppression. The whole system was tested by studying elastic and inelastic scattering of  $^{20}\text{Ne}$  on  $^4\text{He}$  populating high-lying states in  $^{20}\text{Ne}$  which also decay by  $\alpha$  emission. The Q-value resolution of this setup was about 250-keV FWHM mainly determined by the geometry of the detector-target system.

Q-value spectra for  $\alpha$  particles measured in the position sensitive Si detector telescope, in coincidence with either  $^{19}\text{Ne}$  (left) or  $^{15}\text{O}$  (right), are shown in Fig. I-5. The  $^{15}\text{O}$  spectrum is free of background especially in the critical region around  $E_x$

= 4 MeV. The solid lines in Fig. I-5 represent Gaussians for which the location in excitation energy was kept fixed to the values obtained in a high resolution  $^{20}\text{Ne}(^3\text{He},\alpha)^{19}\text{Ne}$  experiment measured at the same c.m. energy.<sup>2</sup>

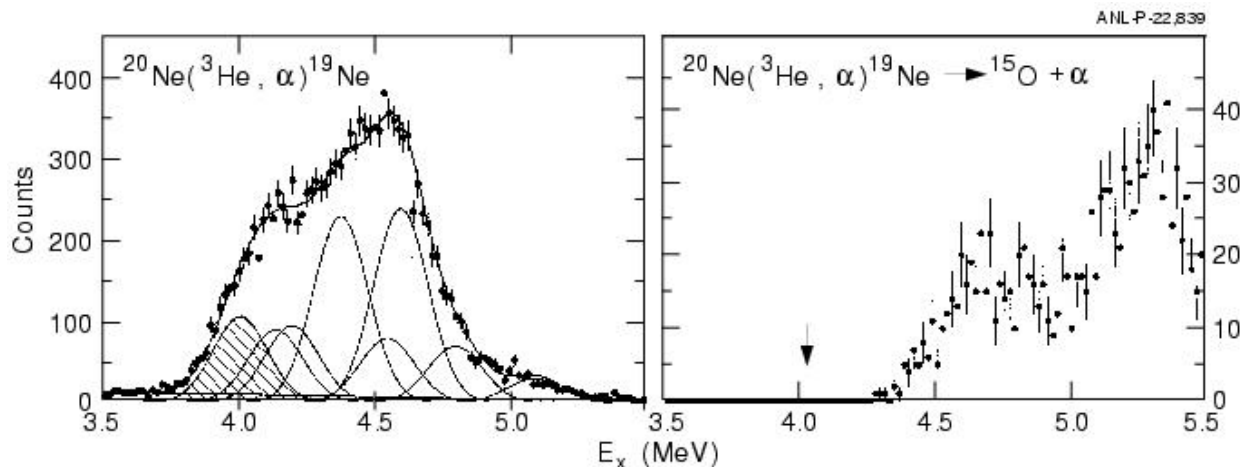


Fig. I-5. Q-value spectra for  $\alpha$  particles in coincidence with  $^{19}\text{Ne}$  (left) or  $^{15}\text{O}$  (right). In both cases the location of the 4.033 MeV state is indicated.

From the two spectra shown in Fig. I-5 upper limits for the branching ratios  $\Gamma_\alpha/\Gamma_\gamma$  for the two astrophysically important states at 4.033 MeV ( $3/2^+$ ) and 4.379 MeV ( $7/2^+$ ) can be deduced. The contribution from the neighboring states at 4.140 ( $9/2^-$ ) and 4.197 ( $7/2^-$ ) MeV is, due to the larger angular momentum transfer, much smaller. Taking into account the detection efficiencies for  $^{15}\text{O}$  and  $^{19}\text{Ne}$  particles transported to the focal plane of the magnetic spectrograph, which was determined from a Monte Carlo calculation, limits of  $\Gamma_\alpha/\Gamma_\gamma \leq 6 \times 10^{-4}$  (4.033 MeV) and  $\leq 1.5 \times 10^{-3}$  (4.379 MeV) were obtained.

From these branching ratios B and the radiative widths  $\Gamma_\gamma$  (typically tens to hundreds of meV) the resonance

strengths  $\omega_\gamma = \omega \frac{\Gamma_\alpha \Gamma_\gamma}{\Gamma_{total}} = \omega \frac{B}{1+B} \Gamma_\gamma$  can be calculated.

For the two important resonances in  $^{19}\text{Ne}$ , good measurements of  $\Gamma_\gamma$  are not yet available. Assuming for  $\Gamma_\gamma$  (4.033 MeV) the limits from Ref. 3 and a theoretical value of  $\Gamma_\gamma = 460 \pm 90$  meV for the 4.379 MeV state,<sup>4</sup> the astrophysical reaction rate for the  $^{15}\text{O}(\alpha,\gamma)$  reaction can be calculated. The results (also including the contributions from higher-lying states) are shown in Fig. I-6.

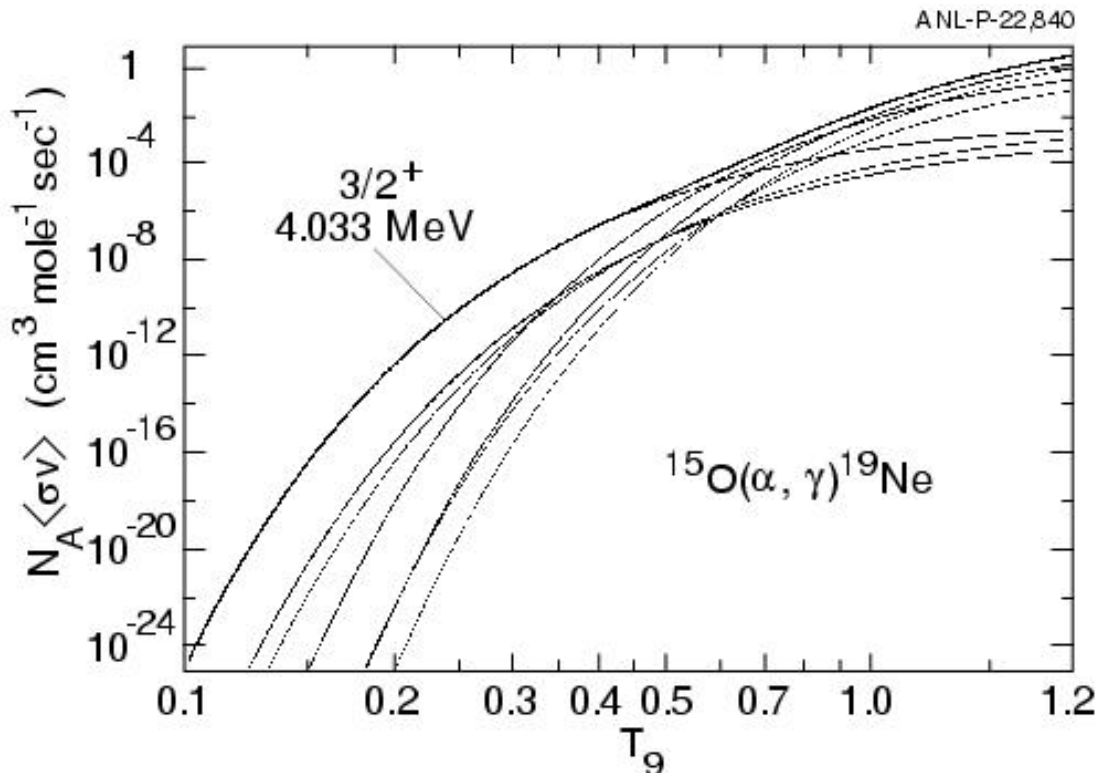


Fig. I-6. Astrophysical reaction rate for the  $^{15}\text{O}(\alpha, \gamma)^{19}\text{Ne}$  reaction.

At low temperatures typical for novae ( $T_9 \sim 0.2 - 0.4$ ), the contribution from the  $3/2^+$  state dominates the reaction rate. Converting the reaction rate into an interaction time, one finds at temperature-density conditions typical of novae  $\rho \sim 10^2 - 10^4 \text{ g/cm}^3$ ,  $T_9 \sim 0.2 - 0.4$ ) values in the regime of  $10^7 - 10^8 \text{ s}$ , i.e. much longer

than the  $\beta$  lifetime of  $^{15}\text{O}$  ( $\tau = 177\text{s}$ ). Thus, no appreciable breakout occurs via the  $^{15}\text{O}(\alpha, \gamma)^{19}\text{Ne}$  reaction in novae. On the surface of accreting neutron stars, i.e. at temperature-densities of  $T_9 \sim 1.5$  and  $\rho \sim 10^4 - 10^7$ , the interaction time is  $\sim 10^{-5} \text{ s}$ , leading to a considerable breakout under these conditions.

\*Northwestern University, †Hebrew University, Jerusalem, Israel.

<sup>1</sup>A. E. Champagne and M. Wiescher, *Annu. Rev. Nucl. Part. Sci.* **42**, 39 (1992).

<sup>2</sup>J. D. Garrett, R. Middleton, and H. T. Fortune, *Phys. Rev. C* **2**, 1243 (1970).

<sup>3</sup>G. Hackman *et al.*, *Phys. Rev. C* **61**, 052801 (2001).

<sup>4</sup>B. A. Brown, private communication.

#### a.4. The Astrophysical Rate of the $^{15}\text{O}(\alpha, \gamma)^{19}\text{Ne}$ Reaction Studied via the $^{21}\text{Ne}(p, t)^{19}\text{Ne}$ Reaction (K. E. Rehm, A. H. Wuosmaa, B. Davids,\* A. M. van den Berg,\* P. Dendooven,\* F. Fleurot,\* M. Hunyadi,\* M. A. de Huu,\* R. H. Siemssen,\* H. W. Wilschut,\* and H. J. Woertche\*)

The  $^{15}\text{O}(\alpha, \gamma)^{19}\text{Ne}$  reaction represents one of the possible breakout paths from the hot CNO cycle into the rp-process. A direct measurement of this reaction, which has an estimated cross section of  $\sim 100 \text{ pb}$ , is currently not feasible because it requires very intense

$^{15}\text{O}$  beams which are not yet available. For this reason, only indirect measurements have been performed so far. In these experiments states in  $^{19}\text{Ne}$  above the  $(\alpha, \gamma)$  threshold are populated by various transfer reactions (e.g.  $^{20}\text{Ne}(^3\text{He}, \alpha)^{19}\text{Ne}$ ) and their branching ratios  $\Gamma_\gamma/\Gamma_\alpha$

measured by identifying the corresponding decay products. The best transfer reaction for populating the first  $3/2^+$  state at 4.033 MeV in  $^{19}\text{Ne}$  which has the strongest influence on the astrophysical reaction rate is the  $^{21}\text{Ne}(p,t)^{19}\text{Ne}$  reaction, which, however, requires high energetic particle beams ( $\geq 20$  MeV/u).

We studied this reaction in inverse kinematics via the reaction  $p(^{21}\text{Ne},t)^{19}\text{Ne}$  with a 43 MeV/u  $^{21}\text{Ne}$  beam from the Kernfysisch Versneller Instituut in Groningen bombarding a  $1 \text{ mg/cm}^2$   $(\text{CH}_2)_n$  target. Both triton ejectiles and  $^{19}\text{Ne}$  recoils entered the Big-Bite Spectrometer which was positioned at  $0^\circ$ . The  $^{19}\text{Ne}$  recoils and  $^{15}\text{O}$  decay products were identified in two

phoswich detectors, which provided energy loss, total energy and timing information. The tritons were identified in a similar array of phoswich detectors after passing through the vertical drift chambers located in the focal plane of the spectrometer. Due to the excellent energy resolution in the spectrometer the branching ratio  $\Gamma_\alpha/\Gamma$  of 6 states above the alpha threshold in  $^{19}\text{Ne}$  could be determined. These values and the resulting  $\alpha$  widths  $\Gamma_\alpha$  (obtained from measured and calculated radiative widths) are summarized in Table I-1. Because of the small value of the  $\alpha$  width the  $^{15}\text{O}(\alpha,\gamma)^{19}\text{Ne}$  reaction does not play a significant role in the breakout from the hot CNO cycle into the rp process in nova explosions.

\*Kernfysisch Versneller Instituut, Groningen, The Netherlands.

Table I-1. Branching ratios  $B_\alpha \equiv \Gamma_\alpha/\Gamma$  and decay widths.

$E_x$ (MeV)	$J^\pi$	$B_\alpha$	$\Gamma_\gamma$ (meV)	$\Gamma_\alpha$ (meV)
4.033	$3/2^+$	$< 4.3 \times 10^{-4}$	$45^{+200}_{-33}$	$< 0.13$
4.379	$7/2^+$	$< 3.9 \times 10^{-3}$	$458 \pm 92$	$< 2.3$
4.549	$(3/2)^-$	$0.16 \pm 0.04$	$39^{+34}_{-15}$	$4.4^{+4.0}_{-2.0}$
4.600	$(5/2^+)$	$0.32 \pm 0.04$	$101 \pm 55$	$43 \pm 24$
4.712	$(5/2^-)$	$0.85 \pm 0.04$	$43 \pm 8$	$230 \pm 80$
5.092	$5/2^+$	$0.90 \pm 0.06$	$107 \pm 17$	$960 \pm 530$

**a.5. On the  $\gamma$  Decay of the 2643-keV State in the rp Breakout Nucleus  $^{20}\text{Na}$**   
 (D. Seweryniak, A. Heinz, R. V. F. Janssens, T. L. Khoo, E. Rehm, P. J. Woods,\*  
 H. Mahmud,\* F. Sarazin,\* J. Goerres,† A. Aprahamian,† M. Shawcross,† J. Shergur,‡  
 M. Wiescher,† and A. Woehr‡)

The reaction sequence  $^{15}\text{O}(\alpha,\gamma)^{19}\text{Ne}(p,\gamma)^{20}\text{Na}$  is thought to be the dominating nucleosynthetic mechanism responsible for breakout from the hot CNO cycles into the rp process. However, neither of these reaction rates has been determined. One of the key uncertainties in the  $^{19}\text{Ne}(p,\gamma)^{20}\text{Na}$  reaction is the structure of the resonance state in  $^{20}\text{Na}$  at an excitation energy of about 2.643 MeV, which is thought to dominate the astrophysical reaction rate. Contradictory  $3^+$  and  $1^+$  assignments were proposed for this state in the literature.

An in-beam  $\gamma$ -ray experiment was performed using the Argonne Fragment Mass Analyzer to study  $\gamma$ -decaying states in  $^{20}\text{Na}$ . The  $^{10}\text{B}(^{12}\text{C}, 2n)$  reaction was used to populate excited states in  $^{20}\text{Na}$ . Gamma rays were detected using 2 Ge clover detectors and a  $4\pi$  array of BGO scintillators placed around the target. Recoiling reaction products were separated from the beam and dispersed according to their mass over charge state ratio in the FMA. Mass-20 residues, selected by the slits at the focal plane of the FMA, were stopped in an ionization chamber and their atomic number was deduced based on the energy loss and energy measurement.

Figure I-7 shows the  $\gamma$ -ray spectrum tagged by  $^{20}\text{Na}$  recoils. The transitions present in this spectrum were placed in the preliminary level scheme shown in Fig. I-8. Figure I-8 shows only the states observed in this work. The energies of the observed  $\gamma$  rays are in agreement with level energies obtained from previous transfer reaction studies. The state depopulated by the 1029 keV  $\gamma$  ray was seen for the first time. Based on the comparison with the mirror  $^{20}\text{F}$  spin  $5^+$  was assigned to this state. A 1237-keV transition is proposed to deexcite a new  $2^+$  state. A  $\gamma$ -ray line can be seen at the energy of about 1851 keV in the inset of Fig. I-7. The energy of this line agrees within experimental errors with the energy difference between the 2643 keV state and the 798 keV state. The BGO spectrum gated by the three bottom transition contains excess of counts around 1800-1900 keV, although the statistics are low (see Fig. I-9). This could imply that the  $3^+$  assignment for the 2643 keV state is more likely than  $1^+$ . However, the 1851-keV transition might deexcite the known  $2^-$  state at 1837(7) keV. To resolve this ambiguity another experiment using Gammasphere was proposed and will be carried out this year.

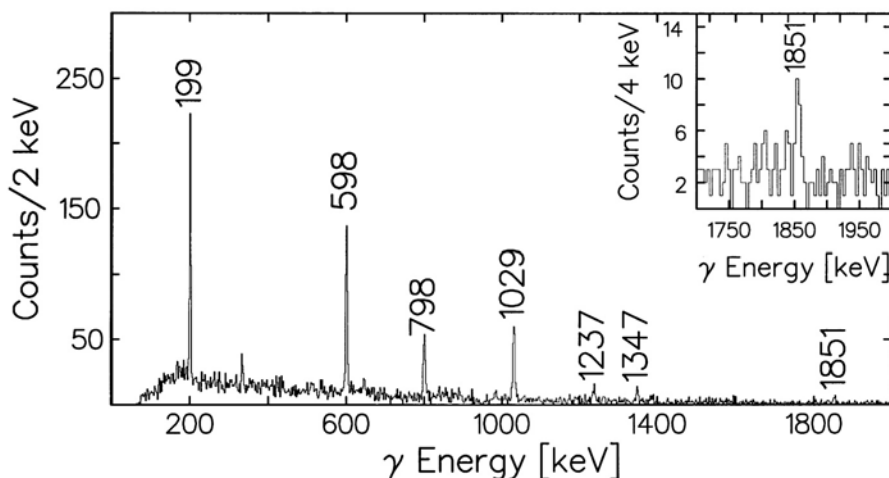


Fig. I-7. Ge  $\gamma$ -ray spectrum measured in coincidence with  $^{20}\text{Na}$  residues.

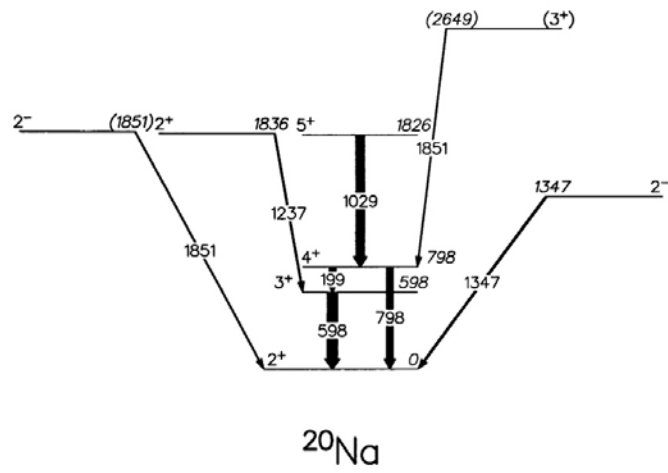


Fig. I-8. Preliminary  $^{20}\text{Na}$  level scheme.

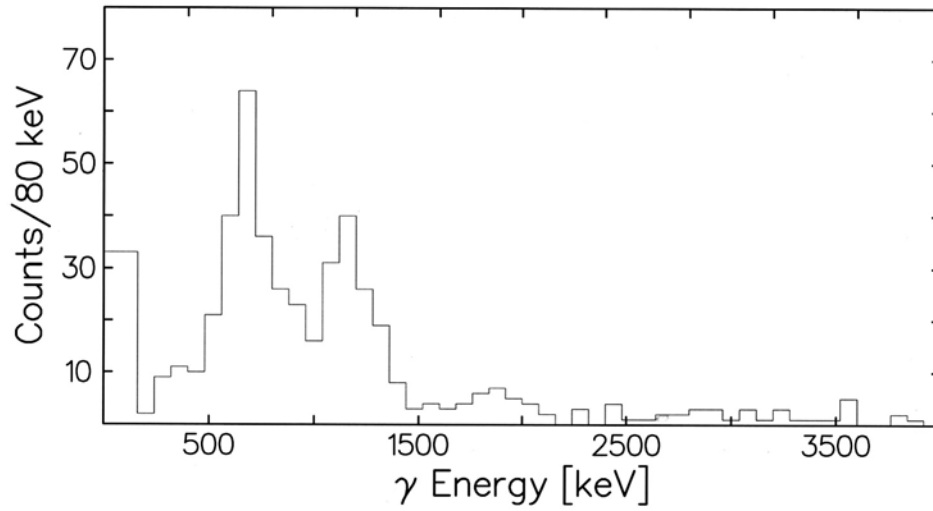


Fig. I-9 BGO  $\gamma$ -ray spectrum gated by the 199 keV, 598 keV and 798 keV Ge gates.

**a.6. Study of the Breakout Reaction  $^{18}\text{Ne}(\alpha,p)^{21}\text{Na}$**  (S. Sinha, J. P. Greene, D. Henderson, R. V. F. Janssens, C. L. Jiang, E. F. Moore, G. Mukherjee, R. C. Pardo, T. Pennington, K. E. Rehm, J. P. Schiffer, S. Artemov,\* A. Chen,† L. Jisonna,‡ R. E. Segel,‡ and A. H. Wuosmaa§)

The breakout from the hot CNO cycle into the rp-process is controlled by three reactions:  $^{18}\text{F}(p,\alpha)^{15}\text{O}$ ,  $^{15}\text{O}(\alpha,\gamma)^{19}\text{Ne}$ , and  $^{18}\text{Ne}(\alpha,p)^{21}\text{Na}$ .<sup>1</sup> The first of these reactions has to compete with the  $^{18}\text{F}(p,\gamma)^{15}\text{O}$  cross section, which is stronger by a factor of about  $2 \times 10^3$ .<sup>2</sup> The second reaction was found to be negligible at nova temperatures, due to the small alpha width of the first excited state above the threshold in  $^{19}\text{Ne}$ . The third reaction has the highest Coulomb barrier among the three possible candidates, but has so far been studied only in the excitation energy region  $E_x(^{22}\text{Mg}) \geq 10.12$  MeV.<sup>3</sup> We performed an experiment with the goal to extend these measurements down to  $E_x = 9.3$  MeV. To avoid the use of a  $^4\text{He}$  gas target we studied the  $(\alpha, p)$  reaction through its time-inverse  $p(^{21}\text{Na}, \alpha)^{18}\text{Ne}$  reaction using a  $^{21}\text{Na}$  beam produced with the in-flight technique. A gas cell target filled with deuterium was bombarded with a  $^{20}\text{Ne}$  beam from ATLAS and the  $^{21}\text{Na}^{11+}$  ions produced via the  $d(^{20}\text{Ne}, ^{21}\text{Na})n$  reaction

were transported into a scattering chamber located in front the Split-pole spectrograph. Beam intensities of  $2 \times 10^5$  Na/s on target were obtained, limited by the amount of  $^{20}\text{Ne}$  beam that could be put on the gas cell foils. The hydrogen target consisted of a  $360\text{-}\mu\text{g}/\text{cm}^2$  thick  $\text{CH}_2$  foil, equivalent to a range of 150 KeV in excitation energy. The outgoing particles ( $^{18}\text{Ne}$  and  $\alpha$ ) were detected in coincidence in a PPAC-ionization chamber—position sensitive Si detector array consisting of two annular strip detectors, providing energy and angle information. This setup also allows us to obtain information about elastic and inelastic scattering of protons on a  $^{21}\text{Na}$  which is needed to obtain the transition strengths to excited states in  $^{21}\text{Na}$  populated via the  $^{18}\text{Ne}(\alpha,p)^{21}\text{Na}$  reaction. With this setup, an excitation function in the energy range  $E_x = 9.3\text{-}10.5$  MeV was measured. The data are presently being analyzed.

\*Institute of Nuclear Physics, Tashkent, Uzbekistan, †McMaster University, Hamilton, Ontario, ‡Northwestern University, §Western Michigan University.

<sup>1</sup>A. E. Champagne and M. Wiescher, *Annu. Rev. Nucl. Part. Sci.* **42**, 39 (1992).

<sup>2</sup>K. E. Rehm *et al.*, *Phys. Rev. C* **55**, R566 (1997).

<sup>3</sup>D. Groombridge *et al.*, *Phys. Rev. C* **66**, 055802 (2002).

**a.7. Ne, Na and Al Burning in Astrophysically Important (p,γ) Reactions** (C. J. Lister, M. P. Carpenter, T. L. Khoo, R. V. F. Janssens, E. F. Moore, G. Mukherjee, K. E. Rehm, A. H. Wuosmaa, D. G. Jenkins,\* B. R. Fulton,† M. Freer,† B. J. Truett,‡ and J. Jose§)

The exact excitation energies, spins, parities and widths of near-threshold states in astrophysically important (p,γ) burning reactions have a very strong impact on the reaction rates which produce and destroy elements. For some time we have been investigating the possibility of using heavy ion reactions to populate these states, and then exploiting the power of Gammasphere to investigate the radiative decays. This approach seems generally very useful in precisely placing the excitation energy of states with “germanium-quality” resolution, (i.e. to a few kilo-electron volts), in resolving close doublets, in constraining spins through angular distribution and branching determinations, and in measuring short lifetimes through the Differential Doppler Shift technique.

Our first project, investigating the  $^{22}\text{Na}(p,\gamma)^{23}\text{Mg}$  reaction through use of the  $^{12}\text{C}(^{12}\text{C},n)^{23}\text{Mg}$  population mechanism, made most progress. We were helped by collaboration with an astrophysicist, Professor J. Jose from the University of Vilanova in Spain, who is interested in production and destruction of intermediate mass isotopes and helped with interpretation of the significance of our new reaction rate determination, and its implication for space-based gamma-ray astronomy. A *Physical Review Letter*<sup>1</sup> was submitted on this subject.

We also collected some data relevant to the  $^{26}\text{Al}(p,\gamma)^{27}\text{Si}$  reaction, through investigation of the  $^{16}\text{O}(^{12}\text{C},n)^{27}\text{Si}$  production mechanism. This destruction reaction is important, as gamma-rays associated with

$^{26}\text{Al}$  beta-decay were seen in space-based observatories, so production and destruction rates are crucial for investigating the amount of  $^{26}\text{Al}$  produced in explosive

cosmic events. It is clear that a new dedicated experiment will be needed to produce the data set required for a useful investigation.

\*University of York, United Kingdom, †University of Birmingham, United Kingdom, ‡Purdue University-Calumet, §University of Vilanova, Spain.

<sup>1</sup>D. G. Jenkins *et al.* submitted to Phys. Rev. Lett. April 2003.

**a.8. Production of a Radioactive  $^{37}\text{K}$  Beam with the In-Flight Technique** (K. E. Rehm, R. C. Pardo, J. P. Greene, A. Heinz, D. Henderson, R. V. F. Janssens, C. L. Jiang, L. Jisonna, E. F. Moore, G. Mukherjee, T. Pennington, J. P. Schiffer, R. E. Segel, and S. Sinha)

In some explosive astrophysical environments the reaction flow proceeds through a series of ( $\alpha$ ,p) reactions or proton-rich nuclei. One of these is the  $^{34}\text{Ar}(\alpha,p)^{37}\text{K}$  reaction which plays an important role for the light curve of x-ray bursts.<sup>1</sup> Earlier plans to measure this reaction directly with a  $^{34}\text{Ar}$  beam and a  $^4\text{He}$  target were unsuccessful due to difficulties with separating the heavy reaction products ( $^{37}\text{K}$ ,  $^{34}\text{Ar}$ ) from the  $^{32}\text{S}$  primary beam which is used to produce the  $^{34}\text{Ar}$  beam. It was, therefore, decided to study the time-inverse  $^{37}\text{K}(p,\alpha)^{34}\text{Ar}$  reaction, and to obtain the necessary information through the principle of detailed balance. The  $^{37}\text{K}$  beam is produced via the inverse  $d(^{36}\text{Ar},^{37}\text{K})n$  reaction with a 300 MeV  $^{36}\text{Ar}$  beam from the ATLAS accelerator bombarding a gas cell target filled with deuterium and cooled to liquid nitrogen

temperatures. The  $^{37}\text{K}^{19+}$  ions ( $E = 260$  MeV) were collected with a superconducting solenoid located directly behind the production target and separated from the primary  $^{36}\text{Ar}$  beam with the  $22^\circ$  bending magnet. The beam intensity and purity were monitored with the position-sensitive ionization chamber located in the focal plane of the magnetic spectrograph. The specific production rate measured at this energy was 1200  $^{37}\text{K}/\text{sec}/(\text{pnA of } ^{36}\text{Ar beam})$ . Although the ATLAS accelerator could provide sufficient  $^{36}\text{Ar}$  intensity to produce secondary beam intensities of  $5 \times 10^5$   $^{37}\text{K}/\text{s}$  on target, the HAVAR entrance and exit foils of the gas target could only withstand a primary beam intensity of 50 pnA. In order to increase this value we plan to replace the foils with a higher melting point material in a future run.

<sup>1</sup>M. Wiescher *et al.*, J. Phys. G **25**, R133 (1999).

**a.9. Measurement of  $^{44}\text{Ti}$  Half-Life** (I. Ahmad, J. P. Greene, E. F. Moore, W. Kutschera,\* and M. Paul†)

The half-life measurement of  $^{44}\text{Ti}$ , which was started in March 1992, is being continued at Argonne and Jerusalem with the aim of reducing systematic uncertainties. The half-life determined from 5 years decay was published<sup>1</sup> in 1998. Now we have data for more than 10 years decay. The half-life is being measured by recording spectra of a mixed source of  $^{44}\text{Ti}$  and  $^{60}\text{Co}$  with a 25% Ge detector at regular intervals. At Argonne, the spectra of the mixed source are being measured at two source-to-detector distances of 5.2 cm and 10.2 cm. Also, spectra of pure  $^{44}\text{Ti}$  and

pure  $^{60}\text{Co}$  are measured separately at 5.2 and 10.2 cm. The half-life values were obtained by analyzing the 1157/1173 and 1157/1333 ratios of the  $^{44}\text{Ti}$  and  $^{60}\text{Co}$  gamma rays. The preliminary analysis shows that the half-life of  $59.2 \pm 0.6$  yr reported in our 1998 article is still correct within the quoted uncertainty. The decay of the 1157/1173 ratio measured for a source-to-detector distance of 5.2 cm is displayed in Fig. I-10 The spectra are being analyzed and the results will be published by the end of the year.

\*University of Vienna, Austria, †Hebrew University, Jerusalem, Israel.

<sup>1</sup>I. Ahmad *et al.*, Phys. Rev. Lett. **80**, 2550 (1998).

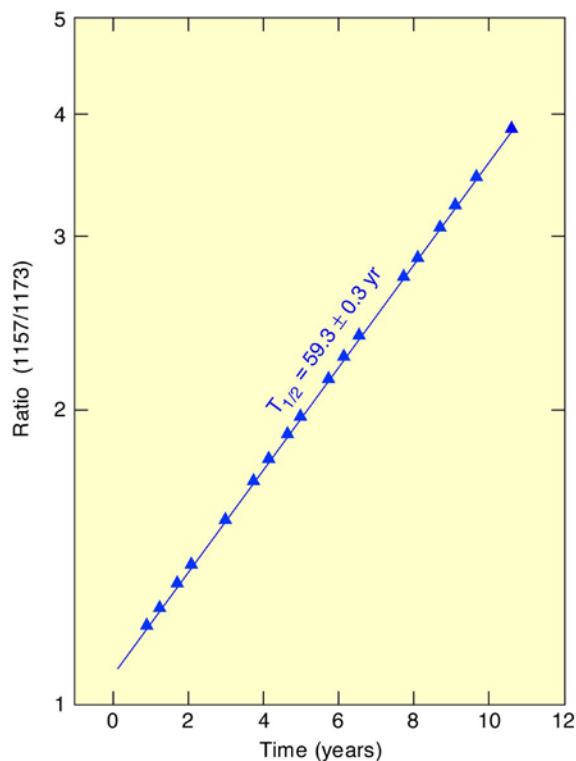


Fig. I-10. A semilogarithmic plot of the ratio of counts in 1157.0-keV peak of  $^{44}\text{Ti}$  and 1173.2-keV peak of  $^{60}\text{Co}$  against decay time. The measurements were performed at ANL using a mixed source of  $^{44}\text{Ti}$  and  $^{60}\text{Co}$ .

**a.10. Mass Measurements Along the rp-Process Using the Canadian Penning Trap Mass Spectrometer** (G. Savard, B. Blank, A. Heinz, A. F. Levand, D. Seweryniak, W. Trimble, Z. Zhou, J. A. Clark,\* J. Vaz,\* J. C. Wang,\* R. C. Barber,† K. S. Sharma,† C. Boudreau,‡ F. Buchinger,§ J. E. Crawford,§ S. Gulick,§ J. K. P. Lee,§ and G. D. Sprouse¶)

A large variety of elements are known to exist in the universe, but the processes that created many of them are not well understood. A possible scenario for their production is a rapid proton-capture process (rp-process<sup>1</sup>), which is thought to occur in such explosive astrophysical events as novae and X-ray bursts. The masses of the nuclides involved are essential in determining the exact path of the rp-process. Particularly important are the masses of "waiting-point" nuclides along the rp-process path where the process stalls until the subsequent  $\beta$ -decay of these nuclides. The masses of two significant waiting-point nuclides, namely  $^{68}\text{Se}$  and  $^{64}\text{Ge}$ , are critical in determining the final abundance of the elements and the light-curve profiles and energy generation of X-ray bursts. For

temperatures of  $10^9$  K which occur on the surface of these stellar environments, a mass precision of at least  $kT/c^2 \sim 100 \text{ keV}/c^2$  is required. Such a precision is obtained easily with the Canadian Penning Trap (CPT) mass spectrometer.

The nuclides investigated are produced in fusion-evaporation reactions between targets mounted on a rotating wheel and heavy-ion beams from the ATLAS facility (see Fig. I-11). Once created, the reaction products are separated from the primary beam using a velocity filter and enter an Enge magnetic spectrograph where they are mass separated and focussed into a gas catcher system. There, the initially high-energy recoil products are thermalized in 200 mbar of helium.

The ions are extracted from the gas cell via a combination of gas flow and electric fields and are guided towards the isobar separator as the helium is pumped away.

It is necessary to limit the number of impurity ions injected into the precision Penning trap. Any contaminants may overwhelm the weakly-produced isotopes of interest and affect the measured cyclotron frequency. The reduction of these contaminant ions is accomplished by the newly installed isobar separator (see report g.10.). The desired ions are then periodically ejected and guided to a radio-frequency quadrupole (RFQ) ion trap where they are accumulated before being transferred to the precision Penning trap.

During the past year, mass measurements of  $^{64}\text{Ge}$  and  $^{68}\text{Se}$  were completed. The production of  $^{68}\text{Se}$  was provided by the reaction between a 220 MeV beam of  $^{58}\text{Ni}$  upon a carbon target. The masses of other nuclides created in this reaction, notably  $^{68}\text{Ge}$  and  $^{68}\text{As}$ , were also measured and improved. Recently, an experiment was conducted to measure the mass of  $^{64}\text{Ge}$ , the resulting TOF spectrum is shown in Fig. I-12. In this case, a 185 MeV  $^{54}\text{Fe}$  beam was incident upon the carbon target. The analysis of  $^{68}\text{Se}$  is almost complete ( $m = 67941798 \pm 35 \mu\text{u}$ ) and a preliminary value for the mass of  $^{64}\text{Ge}$  is  $63941653 \pm 34 \mu\text{u}$ . The influence of these new masses on the duration and intensity of the light curve will now be studied.

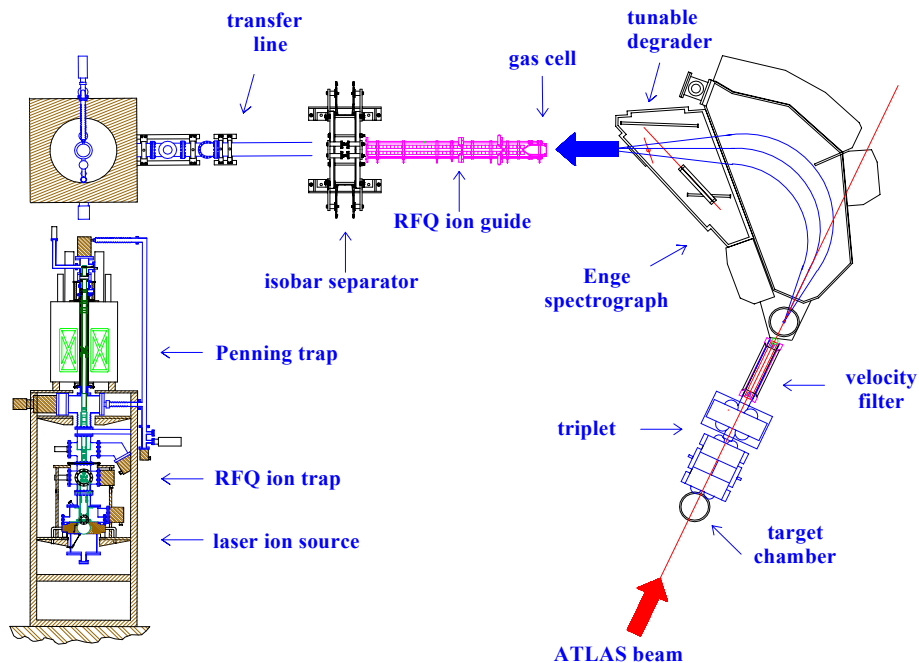


Fig. I-11. An overview of the CPT apparatus, including the recent addition of the isobar separator. The lower left section of the figure is a side view of the CPT.

Attention will now move to the end-point of the rp-process which has been calculated to reach the Sb-Te region and occurs during the cooling phase of the X-ray burst. Mass information is critical as inputs to these calculations. We are therefore setting up for a

measurement of the masses of neutron-deficient Sb and Sn isotopes which dictate the behavior of the alpha-cycling expected to be responsible for the rp-process termination.

\*Argonne National Laboratory and University of Manitoba, Winnipeg, Manitoba, †University of Manitoba, Winnipeg, Manitoba, ‡Argonne National Laboratory and McGill University, Montreal, Quebec, §McGill University, Montreal, Quebec, ¶State University of New York at Stony Brook.

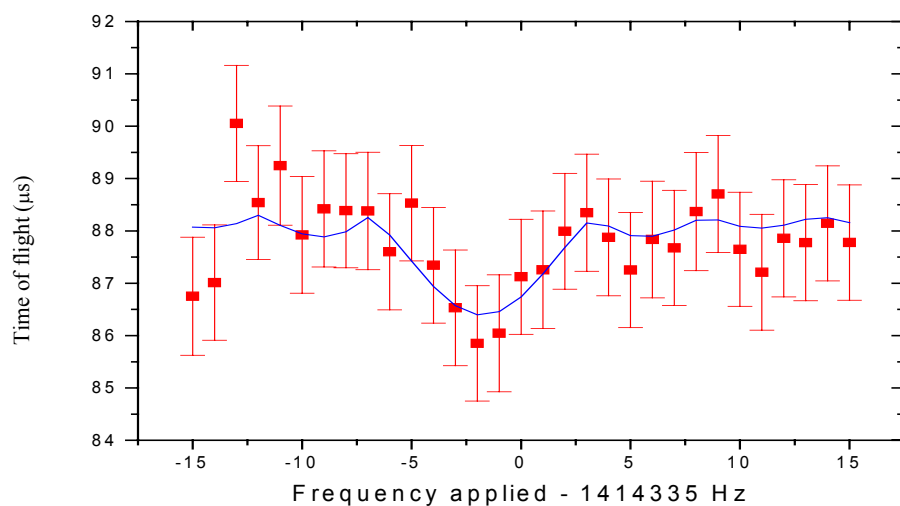


Fig. I-12. Time-of-flight spectrum for  $^{64}\text{Ge}$  ions. The ions excited at resonance gain energy and hence exhibit a slightly shorter flight time in transit to the detector.

**a.11. Direct  $Q_{\beta}$  Measurement of the  $N = Z$  rp-Process Waiting-Point Nucleus  $^{68}\text{Se}$  and Its Astrophysical Implications** (A. Wöhr,<sup>\*</sup> C. N. Davids, A. M. Heinz, R. F. V Janssens, D. Seweryniak, S. M. Fischer,<sup>†</sup> A. Arahamian,<sup>‡</sup> P. Boutachkov,<sup>‡</sup> D. S. Brenner,<sup>§</sup> J. L. Galache,<sup>‡</sup> J. Görres,<sup>‡</sup> A. Teyrurazyan,<sup>‡</sup> M. Shawcross,<sup>‡</sup> and M. C. Wiescher<sup>‡</sup>)

The motivation of this experiment is the behavior of the rp-process at the  $^{68}\text{Se}$ -waiting point (see Fig. I-13). The question is, whether the waiting point is overcome by  $\beta$ -decay into  $^{68}\text{As}$  or by the reaction  $^{68}\text{Se}(2p,\gamma)^{70}\text{Kr}$ . One tile in this jigsaw puzzle is the mass of  $^{68}\text{Se}$ , which is deduced via  $\beta$ -endpoint measurement. This endpoint was measured at the Fragment Mass Analyzer at Argonne National Laboratory using a moving tape collector system. The reaction which was used was  $^{12}\text{C}(^{58}\text{Ni},2n)^{68}\text{Se}$ . Since  $^{68}\text{Se}$  was produced three orders of magnitude less in yield than its isobar  $^{68}\text{As}$ , the analysis proved to be difficult.

The analysis is close to being finished and a publication is in preparation. A preliminary  $Q_{\beta}$  value could be

determined (see Fig. I-14). This value is in agreement with the prediction of Audi and Wapsta. Theoretical calculations performed during the analysis process indicate that there might be an isomer in  $^{68}\text{Se}$ . In previous experiments including this one the predicted isomer could not be observed. Presently an experiment to search for the isomer in  $^{68}\text{Se}$  using the inverse reaction is in preparation at the Notre Dame Nuclear Structure Laboratory.

Furthermore, network calculations to study the influence of different nuclear masses on the rp-process are under way.

<sup>\*</sup>Argonne National Laboratory, University of Notre Dame and University of Maryland, <sup>†</sup>Argonne National Laboratory and DePaul University, <sup>‡</sup>University of Notre Dame, <sup>§</sup>Clark University.

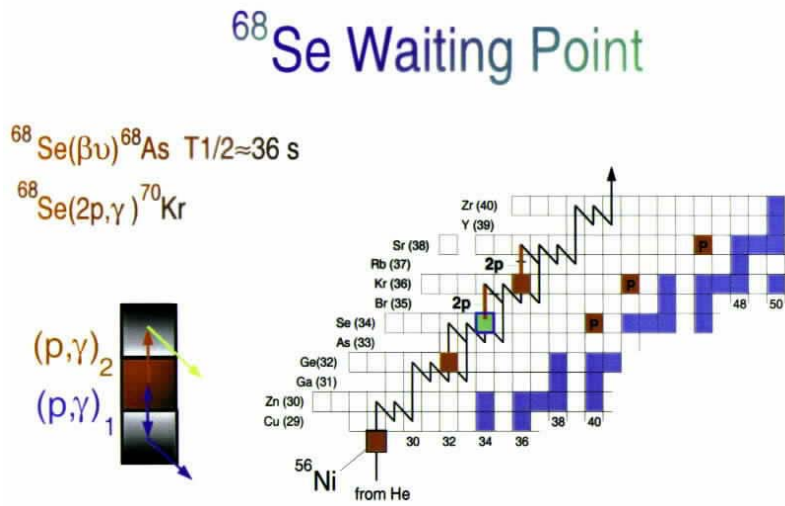


Fig. I-13. The  $N = Z$  rp-process  $^{68}\text{Se}$  waiting point is shown. Possible nucleosynthesis reactions are indicated. The "waiting point" nuclei are very important for setting the timescale for x-ray bursts.

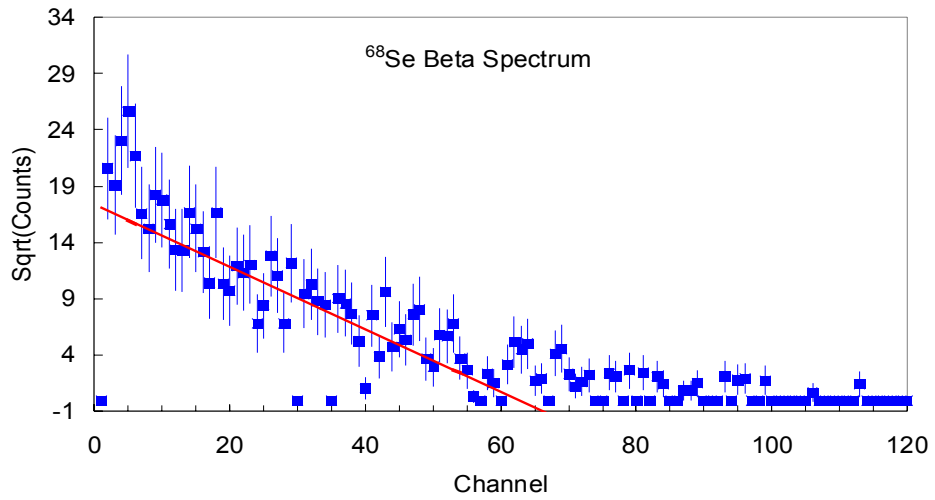


Fig. I-14. Fermi-Kuri plot of the  $^{68}\text{Se}$   $\beta$ -spectrum. Shown here is the sum of all gates feeding the 426 keV level in  $^{68}\text{As}$ .

